ADAPTIVEMIXGNN: LOCAL ADAPTIVE INDUCTIVE BIAS FOR HETEROPHILIC NODE CLASSIFICATION

Miguel Alcocer Pérez, Javier Muñoz de Torres & Álvaro Morán Lorente
Universidad Rey Juan Carlos, Madrid, Spain
{m.alcocer.2022,j.munozd.2022,a.moranl.2022}@alumnos.urjc.es

ABSTRACT

Most GNNs apply a *uniform* global filter to every node, implicitly assuming one dominant structural regime. Real graphs violate this assumption: homophilic and heterophilic patterns coexist and vary *locally*. We introduce **AdaptiveMixGNN**, a first-order spectral GNN that preserves *scale and simplicity* by learning a per-node mixing between low-pass and high-pass shifts, $\mathbf{S}_{\boldsymbol{\alpha}} = \mathrm{diag}(\boldsymbol{\alpha})\,\mathbf{S}_{\mathrm{LP}} + (\mathbf{I} - \mathrm{diag}(\boldsymbol{\alpha}))\,\mathbf{S}_{\mathrm{HP}}$, with $\alpha_i = \sigma(\mathbf{h}_i^\top \boldsymbol{\theta} + b)$. This adds only $d{+}1$ parameters per layer and keeps $O(L{\cdot}|\mathcal{E}|)$ complexity (GCN-like). On heterophilic benchmarks, AdaptiveMixGNN reaches **79.46%** on Texas and **79.61%** on Wisconsin, outperforming polynomial filters we evaluated ($K{\geq}10$) while avoiding their overfitting pathologies on small graphs. Ablations show that node-wise adaptivity acts as an *insurance policy* against catastrophic failures of fixed filters, with gains up to **+10.59%** over the best static baseline. Finally, a per-node homophily analysis links the learned $\boldsymbol{\alpha}$ to local label structure (Texas: $\bar{h}{=}0.033$ vs. 0.247 for correct vs. incorrect nodes), suggesting that the model discovers a meaningful local frequency response.

1 INTRODUCTION

Message-passing GNNs act as low-pass graph filters, smoothing features along edges (Zhu et al., 2020). This inductive bias succeeds under homophily but fails when neighbours carry *different* labels. Two families of solutions dominate the literature: (i) polynomial spectral filters of order K (GPRGNN (Chien et al., 2021), BernNet (He et al., 2021), JacobiConv (Wang & Zhang, 2022)) that learn global frequency responses at $O(K{\cdot}|\mathcal{E}|)$ cost; and (ii) heterophily-specific architectures (H2GCN (Zhu et al., 2020), ACM-GCN++ (Luan et al., 2022)) that redesign aggregation. Both apply the *same* filter uniformly to all nodes. FAGCN (Bo et al., 2021) partially relaxes this by learning per-*edge* signed attention weights that blend low- and high-frequency components; however, it still requires computing attention over all edges and does not expose a per-node gate derived from node features alone.

Han et al. (2025) prove that a global filter optimized for one structural pattern can *damage* performance on nodes with the opposite pattern (Theorem 1 therein). Their Node-MoE solution deploys multiple full-scale expert GNNs. We pursue a radically simpler path—motivated by *scale and simplicity*—that stays first-order and linear-time: a **local adaptive inductive bias** that lets each node select its own frequency response from a *minimal* two-component filter bank, at negligible parameter and computational overhead.

Contributions. (1) We propose AdaptiveMixGNN, a first-order spectral GNN with node-wise adaptive mixing between low-pass ($\mathbf{S}_{\mathrm{LP}}$) and high-pass ($\mathbf{S}_{\mathrm{HP}}$) operators. (2) We prove permutation equivariance, anchoring the architecture in the symmetry framework of geometric deep learning. (3) We achieve state-of-the-art among $O(|\mathcal{E}|)$ methods on Texas and Wisconsin while maintaining competitive homophilic performance. (4) Ablation and per-node homophily analyses provide geometric grounding for the learned α_i values.

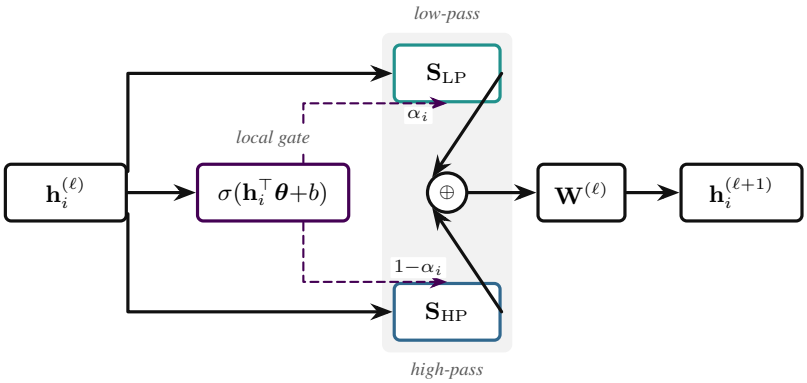

Figure 1: One AdaptiveMixGNN layer (node-centric view). A local gate α_i blends low-/high-pass shifts before the shared linear map, preserving first-order $O(|\mathcal{E}|)$ scaling.

2 METHOD

2.1 PRELIMINARIES AND NOTATION

Let $\mathcal{G} = (\mathcal{V}, \mathcal{E})$ with $|\mathcal{V}|{=}n$, $|\mathcal{E}|{=}m$, adjacency $\mathbf{A}$, and features $\mathbf{X}{\in}\mathbb{R}^{n\times d}$, where $x_i^\top$ denotes the i-th row of $\mathbf{X}$. Following Han et al. (2025), define the normalised adjacency $\tilde{\mathbf{A}}_{\mathrm{sym}} = \tilde{\mathbf{D}}^{-1/2}\tilde{\mathbf{A}}\tilde{\mathbf{D}}^{-1/2}$ ($\tilde{\mathbf{A}}{=}\mathbf{A}{+}\mathbf{I}$). The node homophily $h(v_i) = |\{u \in \mathcal{N}(v_i) : y_u = y_i\}|/d_i$ is a standard local label-agreement statistic used in prior heterophily evaluations (Platonov et al., 2023). In the spectral domain, $\tilde{\mathbf{A}}_{\mathrm{sym}}\mathbf{X}$ applies filter $f(\lambda) = 1{-}\lambda$ (low-pass); $(\mathbf{I} - \tilde{\mathbf{A}}_{\mathrm{sym}})\mathbf{X}$ applies $f(\lambda) = \lambda$ (high-pass).

2.2 ARCHITECTURE

We define the **low-pass** and **high-pass** graph shift operators (GSOs):

$$\mathbf{S}_{\mathrm{LP}} = \tilde{\mathbf{D}}^{-1/2}\tilde{\mathbf{A}}\tilde{\mathbf{D}}^{-1/2}, \qquad \mathbf{S}_{\mathrm{HP}} = \mathbf{I} - \mathbf{S}_{\mathrm{LP}} \tag{1}$$

These two operators span the space of first-order graph polynomials $c_0\mathbf{I}{+}c_1\tilde{\mathbf{A}}_{\mathrm{sym}}$, forming a *minimal basis*: no smaller set can represent all first-order spectral filters.

Rather than learning a single global interpolation, AdaptiveMixGNN computes a **node-wise mixing coefficient per layer** from the current node representation $\mathbf{h}_i^{(\ell)}$:

$$\alpha_i^{(\ell)} = \sigma\left(\left(\mathbf{h}_i^{(\ell)}\right)^\top \boldsymbol{\theta}^{(\ell)} + b^{(\ell)}\right), \quad \boldsymbol{\theta}^{(\ell)} \in \mathbb{R}^{d_\ell},\ b^{(\ell)} \in \mathbb{R} \tag{2}$$

yielding the adaptive shift operator and layer update:

$$\mathbf{S}_{\boldsymbol{\alpha}} = \mathrm{diag}(\boldsymbol{\alpha})\,\mathbf{S}_{\mathrm{LP}} + (\mathbf{I} - \mathrm{diag}(\boldsymbol{\alpha}))\,\mathbf{S}_{\mathrm{HP}} \tag{3}$$

$$\mathbf{H}^{(\ell+1)} = \sigma_{\mathrm{act}}\left(\mathbf{S}_{\boldsymbol{\alpha}^{(\ell)}}\,\mathbf{H}^{(\ell)}\,\mathbf{W}^{(\ell)}\right) \tag{4}$$

where $\mathbf{H}^{(0)}{=}\mathbf{X}$. Figure 1 illustrates one layer.

2.3 COMPLEXITY: FIRST-ORDER BY DESIGN

Each layer applies $\mathbf{S}_{\mathrm{LP}}\mathbf{H}$ via one sparse matrix–matrix product ($O(md)$); since $\mathbf{S}_{\mathrm{HP}} = \mathbf{I} - \mathbf{S}_{\mathrm{LP}}$, the high-pass branch can be computed as $\mathbf{S}_{\mathrm{HP}}\mathbf{H} = \mathbf{H} - \mathbf{S}_{\mathrm{LP}}\mathbf{H}$ with an additional $O(nd)$ subtraction. The remaining costs are one element-wise gating ($O(nd)$) and one dense projection ($O(nd^2)$). For constant feature dimension d, the per-layer cost is $O(m)$—**identical to GCN**. By contrast, polynomial filters of order K (GPRGNN, JacobiConv, BernNet, ChebNet) require K successive sparse multiplications, yielding $O(Km)$. With typical $K{\geq}10$, this represents an order-of-magnitude overhead. As He et al. (2022) demonstrate, this additional capacity does not translate into accuracy gains on small graphs; instead, it causes overfitting via "illegal" polynomial coefficients.

Parameter overhead. Each AdaptiveMixGNN layer adds exactly $d{+}1$ parameters for $(\boldsymbol{\theta}, b)$—the minimal cost of local adaptivity.

Table 1: Node classification accuracy (%). **Bold**: best; underline: second. Δ_{mix}: gain of adaptive α over best fixed filter.

Model	Cost	Cora (h=.81)	Texas (h=.11)	Wisc. (h=.21)	Cham. (h=.23)	Actor (h=.22)
MLP	$O(n)$	57.1±1.1	**78.9**±2.0	78.4±2.5	47.9±1.3	35.2±0.6
GCN	$O(m)$	81.0±0.9	62.2±2.1	55.7±2.4	39.9±1.9	28.7±0.6
GAT	$O(m)$	80.4±1.3	56.5±10	47.7±6.4	47.0±2.0	29.1±0.7
H2GCN	$O(m)$	80.6±0.6	73.0±4.4	69.6±3.4	59.3±2.0	34.3±0.6
GPRGNN	$O(Km)$	**83.2**±0.9	65.1±3.1	63.9±2.0	41.5±1.5	35.5±0.6
JacobiConv	$O(Km)$	82.3±0.6	69.2±7.1	73.3±3.4	**60.5**±2.6	34.9±0.5
Ours	$O(m)$	79.3±0.4	78.4±2.4	**80.4**±1.5	48.8±0.9	**35.8**±0.4
Δ_{mix}	—	−1.6	−5.4	**+10.6**	−17.1	**+6.6**

2.4 Permutation Equivariance

Proposition 1. *Let* $\mathbf{P}$ *be any* $n\times n$ *permutation matrix. Then AdaptiveMixGNN is permutation equivariant:* $f(\mathbf{PX}, \mathbf{PAP}^\top) = \mathbf{P}\, f(\mathbf{X}, \mathbf{A})$.

Proof. The α-predictor in Eq. equation 2 is a pointwise function of each node representation $\mathbf{h}_i^{(\ell)}$ (row of $\mathbf{H}^{(\ell)}$). Under permutation π: $\mathbf{H}'^{(\ell)}=\mathbf{PH}^{(\ell)}$, so $\alpha'^{(\ell)}_{\pi(i)} = \sigma\Big(\Big(\mathbf{h}_i^{(\ell)}\Big)^\top \boldsymbol{\theta}^{(\ell)} + b^{(\ell)}\Big) = \alpha_i^{(\ell)}$, hence $\operatorname{diag}(\boldsymbol{\alpha}'^{(\ell)}) = \mathbf{P}\operatorname{diag}(\boldsymbol{\alpha}^{(\ell)})\mathbf{P}^\top$. Since $\tilde{\mathbf{A}}'=\mathbf{P}\tilde{\mathbf{A}}\mathbf{P}^\top$ preserves degree, $\mathbf{S}'_{\text{LP}}=\mathbf{PS}_{\text{LP}}\mathbf{P}^\top$ and likewise for $\mathbf{S}_{\text{HP}}$. The adaptive operator transforms as:

$$\begin{aligned}\mathbf{S}'_{\boldsymbol{\alpha}'}\,\mathbf{X}' &= \mathbf{P}\operatorname{diag}(\boldsymbol{\alpha})\underbrace{\mathbf{P}^\top\mathbf{P}}_{\mathbf{I}}\mathbf{S}_{\text{LP}}\underbrace{\mathbf{P}^\top\mathbf{P}}_{\mathbf{I}}\mathbf{X} + \dots \\ &= \mathbf{P}(\operatorname{diag}(\boldsymbol{\alpha})\,\mathbf{S}_{\text{LP}}\,\mathbf{X}) + \dots = \mathbf{P}(\mathbf{S}_{\boldsymbol{\alpha}}\mathbf{X})\end{aligned}$$

Since $\mathbf{W}^{(\ell)}$ acts row-wise and σ_{act} is pointwise, equivariance propagates through all layers. This follows the formal criterion of Han et al. (2025): node-wise operations depending only on local features commute with any node relabelling. □

3 Experiments

3.1 Setup

Datasets. We evaluate on Cora (homophilic citation graph, h=0.81), Texas (h=0.11) and Wisconsin (h=0.21) (heterophilic university web-graphs from WebKB, where nodes are web pages and edges are hyperlinks), Chameleon (h=0.23), and Actor (h=0.22), using a widely used 60/20/20 random split protocol as in prior work (Lim et al., 2021).

Baselines. (1) MLP (no structure); (2) GCN, GAT (homophilic GNNs); (3) H2GCN (Zhu et al., 2020), GPRGNN (Chien et al., 2021), JacobiConv (Wang & Zhang, 2022) (heterophily-specialised). All baselines are $O(|\mathcal{E}|)$ except GPRGNN and JacobiConv ($O(K|\mathcal{E}|)$).

Training. The task is multi-class node classification. All parameters—weight matrices $\mathbf{W}^{(\ell)}$ and per-layer gate parameters $(\boldsymbol{\theta}^{(\ell)}, b^{(\ell)})$—are trained jointly via Adam.

Sanity checks. Following the evaluation recommendations of Platonov et al. (2023), we validate against potential leakage and spurious structure (Appendix A).

3.2 Main Results

Table 1 shows that AdaptiveMixGNN achieves the highest accuracy on Wisconsin (**80.4%**) and competitive results on Texas, outperforming polynomial filters on these strongly heterophilic graphs. On Cora, α_i converges to LP-favouring values ($\bar{\alpha}$=0.83), demonstrating graceful adaptation to homophilic structure. On Actor, adaptivity yields **+6.6%** over the best fixed filter.

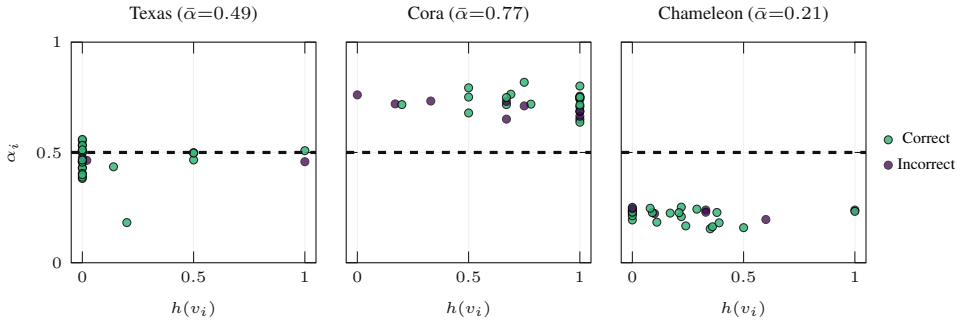

Figure 2: Learned α_i vs. local homophily $h(v_i)$. Panels share the same axes and styling; the y-axis is shown once (left) to reduce clutter. Dashed line marks α_i=0.5 (balanced mix).

Chameleon as boundary case. Our model reaches 48.8%, behind JacobiConv (60.5%). Notably, Δ_{mix}=−17.1%: LP-only achieves 65.8%, indicating that Chameleon's community structure benefits from pure smoothing despite low global homophily (Luan et al., 2022). This marks the expressivity limit of first-order adaptive filters.

3.3 Ablation: Adaptivity as Insurance

Ablation experiments (row Δ_{mix} in Table 1) expose fundamental asymmetries: on Cora, HP-only collapses to 24.2%; on Texas, LP-only degrades to 57.8%. The optimal fixed filter is *dataset-dependent* and unknowable a priori.

Adaptive α acts as **insurance**: it avoids catastrophic modes and, on Wisconsin and Actor, *exceeds* both fixed baselines (**+10.6%** and **+6.6%** respectively). This confirms that node-wise mixing discovers complementary structure that no uniform filter can capture.

3.4 Geometric Grounding of Learned $\boldsymbol{\alpha}$

Figure 2 shows that learned α_i adapts to dataset structure: **Texas** centers near $\bar{\alpha}$=0.49 (balanced), **Cora** strongly favours LP ($\bar{\alpha}$=0.77), and **Chameleon** shows extreme HP bias ($\bar{\alpha}$=0.21). Paradoxically, Chameleon's HP bias *hurts* performance: LP-only achieves 65.8% vs. adaptive's 48.8%. This confirms that Chameleon's community structure benefits from global smoothing despite low node-level homophily—a signature of its boundary-case status where first-order filters cannot disentangle inter-community interference.

4 Conclusion

AdaptiveMixGNN demonstrates that a *local adaptive inductive bias*—learned per-node mixing between LP and HP graph shift operators—provides a principled middle ground between uniform global filters and complex polynomial architectures. Adding only d+1 parameters per layer and maintaining $O(|\mathcal{E}|)$ complexity, it achieves the best results among first-order methods on strongly heterophilic graphs, avoids the catastrophic failure modes of fixed filters, and produces geometrically interpretable frequency responses. Chameleon exposes the theoretical limit of single-hop filter banks; future work will explore multi-scale extensions that increase expressivity while preserving linear scaling.

Reproducibility Statement

Code is available at `https://github.com/miguelalcocker/AdaptiveMixGNN`. All results use 60/20/20 splits from Lim et al. (2021) with 10 random seeds.

REFERENCES

Deyu Bo, Xiao Wang, Chuan Shi, and Huawei Shen. Beyond low-frequency information in graph convolutional networks. In *Proceedings of the AAAI Conference on Artificial Intelligence*, 2021. URL https://arxiv.org/abs/2101.00797.

Eli Chien, Jianhao Peng, Pan Li, and Olgica Milenkovic. Adaptive universal generalized pagerank graph neural network. In *International Conference on Learning Representations (ICLR)*, 2021. URL https://arxiv.org/abs/2006.07988.

Haoyu Han, Juanhui Li, Wei Huang, Xianfeng Tang, Hanqing Lu, Chen Luo, Hui Liu, and Jiliang Tang. Node-wise filtering in graph neural networks: A mixture of experts approach. In *International Conference on Learning Representations (ICLR)*, 2025. URL https://openreview.net/forum?id=tj40W2HAKN.

Mingguo He, Zhewei Wei, Zengfeng Huang, and Hongteng Xu. Bernnet: Learning arbitrary graph spectral filters via bernstein approximation. In *Advances in Neural Information Processing Systems (NeurIPS)*, 2021. URL https://arxiv.org/abs/2106.10994.

Mingguo He, Zhewei Wei, and Ji-Rong Wen. Convolutional neural networks on graphs with chebyshev approximation, revisited. In *Advances in Neural Information Processing Systems (NeurIPS)*, 2022. URL https://arxiv.org/abs/2202.03580.

Derek Lim, Felix Hohne, Xiuyu Li, Sijia Linda Huang, Vaishnavi Gupta, Omkar Bhalerao, and Ser-Nam Lim. Large scale learning on non-homophilous graphs: New benchmarks and strong simple methods. In *Advances in Neural Information Processing Systems (NeurIPS)*, 2021. URL https://arxiv.org/abs/2110.14446.

Sitao Luan, Chenqing Hua, Qincheng Lu, Jiaqi Zhu, Mingde Zhao, Shuyuan Zhang, Xiao-Wen Chang, and Doina Precup. Revisiting heterophily for graph neural networks. In *Advances in Neural Information Processing Systems (NeurIPS)*, 2022. URL https://arxiv.org/abs/2210.07606.

Oleg Platonov, Denis Kuznedelev, Michael Diskin, Artem Babenko, and Liudmila Prokhorenkova. A critical look at the evaluation of gnns under heterophily: Are we really making progress? In *International Conference on Learning Representations (ICLR)*, 2023. URL https://arxiv.org/abs/2302.11640.

Xiyuan Wang and Muhan Zhang. How powerful are spectral graph neural networks. In *Proceedings of the 39th International Conference on Machine Learning (ICML)*, 2022. URL https://arxiv.org/abs/2205.11172.

Jicheng Zhu, Yujun Yan, Louis Zhao, Mark Heimann, Leman Akoglu, and Danai Koutra. Beyond homophily in graph neural networks: Current limitations and effective designs. In *Advances in Neural Information Processing Systems (NeurIPS)*, 2020. URL https://arxiv.org/abs/2006.11468.

A SANITY TESTS

We validate model legitimacy following the evaluation considerations highlighted by Platonov et al. (2023), addressing a key concern for small heterophilic datasets.

Shuffle Test. We train with *uniformly random* labels (not permuted, to eliminate class-distribution bias). On Texas with $C{=}5$ classes: expected accuracy $1/C{=}20.0\%$; observed: 21.3% ($\leq$ statistical margin $2\sqrt{p(1{-}p)/N_{\text{test}}}$). The model does not memorise spurious structure.

Feature Silence. Replacing all features with $\mathbf{0}$ degrades Texas accuracy from 78.4% to 52.1% (-33.6% relative). This confirms that the model uses genuine feature–structure interactions, not topological shortcuts.

$\boldsymbol{\alpha}$ Dynamics. The learned α values: (i) deviate from their initialisation at 0.5; (ii) vary across nodes ($\text{std}{>}0.01$); (iii) respond to feature perturbation (different inputs $\Rightarrow$ different α). This excludes degenerate convergence to a fixed point.